Oil displacement through a porous medium with a temperature gradient

Cláudio L. N. Oliveira,[1,2] José S. Andrade, Jr.,[1,2] and Hans J. Herrmann[1,2]

[1]*Departamento de Física, Universidade Federal do Ceará, Caixa Postal 6030, Campus do Pici, BR-60451-970 Fortaleza, Ceará, Brazil*
[2]*Computational Physics, IfB, ETH Zürich, Hönggerberg, CH-8093 Zürich, Switzerland*

We investigate the effect of a temperature gradient on oil recovery in a two-dimensional pore-network model. The oil viscosity depends on temperature as $\mu_o \propto e^{B/T}$, where B is a physicochemical parameter, depending on the type of oil, and T is the temperature. A temperature gradient is applied across the medium in the flow direction. Initially, the porous medium is saturated with oil, and then another fluid is injected. We have considered two cases representing different injection strategies. In the first case, the invading fluid viscosity is constant (finite viscosity ratio), while in the second one, the invading fluid is inviscid (infinite viscosity ratio). Our results show that for the case of finite viscosity ratio, recovery increases with ΔT independent of strength or sign of the gradient. For an infinite viscosity ratio, a positive temperature gradient is necessary to enhance recovery. Moreover, we show that for $\Delta T > 0$, the percentage of oil recovery generally decreases (increases) with B for a finite (infinite) viscosity ratio. Finally, we also extend our results for infinite viscosity ratio to a three-dimensional porous media geometry.

I. INTRODUCTION

Thermal recovery processes have been used by petroleum companies as a strategic method to improve oil production from reservoirs. These processes consist, basically, in decreasing the oil viscosity (increasing the pressure) by increasing the temperature of the reservoir using a heat source [1]. In practice, this can be done by injecting a hot fluid (steam or water) into the reservoir. A method often called steam or hot-water injection has been mostly used by companies exploiting heavy oil reservoirs [2,3].

The oil viscosity is described by an exponential dependency of temperature allowing a reduction of oil viscosity by several orders of magnitude with only a modest increase of temperature [1]. In general, oil properties in the operational conditions of a reservoir field are very difficult to predict and can be very different for each type of oil or oil mixture. Therefore, their direct measurement is highly desirable for a better understanding of this phenomenon and to improve the efficiency of the recovery.

Several approaches to model and simulate oil recovery have been utilized in the past. Some of them make use of the macroscopic description of conservation laws in a porous medium, simulating a whole reservoir, including injector and producer wells [5,6]. Other authors use conservation laws under a more microscopic approach [7–20], where a portion of the porous medium can be represented by tubes connected to one another. The fluid flow in each tube is easily computed by the Hagen-Pouseille equation. For instance, Lu *et al.* [21–23] have used this type of modeling approach to simulate oil burning by air injection. This represents another thermal recovery method, where the heat source is the burning oil itself. In their work, they have studied the penetration of the burning front into a solid oil phase.

In the present work, we study the displacement in a porous medium of oil with temperature-dependent viscosity being pushed by another fluid. We adopt a simple two-dimensional network model [24–27] previously developed to simulate two-phase flow with arbitrary viscosity ratio. Despite its simplicity, the model is capable of reproducing a large variety of experimental results [24]. In order to adapt this model to our purpose, we implement a temperature gradient in the injection direction and assume that the oil viscosity has an Arrhenius-type dependency on temperature [4]. We studied two different cases according to the viscosity ratio. In the first one, the invading fluid viscosity is constant (finite viscosity ratio) and in the second one, the invading fluid is inviscid (infinite viscosity ratio). The aim of this work is then to investigate the influence of a temperature gradient on the efficiency of oil recovery under these different conditions.

II. MODEL FORMULATION

The porous medium, represented by links and nodes elements, is microscopically disordered, but macroscopically homogenous [28]. The links correspond to pieces of rock of equal length ℓ and cross-section area A. To each link we assign a permeability k, which is a coarse-grain flow property of the pore space, chosen randomly according to a uniform distribution between 25 md and 10 D (1 D $\equiv 10^{-12}$ m^2). This range is typical of rock permeabilities found in oil reservoirs [2]. This randomness in the permeability represents the disorder of the porous medium. The nodes where four links meet are assumed to have no volume. The links are placed on a square lattice tilted by 45° which assures that all links are geometrically equivalent with regard to the average flow, i.e., the links are neither parallel nor perpendicular to the flow direction. Initially, the porous medium is fully saturated with oil and periodic boundary conditions are applied at the top and bottom of the system. The penetration process starts with an invading fluid being injected at a constant flow rate through the left boundary of the system.

The volumetric flow rate in a link connecting neighbor nodes i and j is given by Darcy's law,

$$q_{ij} = -\frac{Ak_{ij}}{\mu_{\text{ef}}}\frac{(p_j - p_i)}{\ell},\tag{1}$$

where p_i is the pressure at node i and k_{ij} is the permeability of the link. The effective viscosity μ_{ef} for a given link is calculated according to a linear mixing rule, namely, $\mu_{\mathrm{ef}} = S_o \mu_o + S_{\mathrm{inv}} \mu_{\mathrm{inv}}$, where S_o and S_{inv} are the saturations of the oil and the invading fluid, respectively, and μ_o and μ_{inv} are their corresponding viscosities. For each species, the saturation is calculated at a link as the volume fraction of the corresponding phase. We assume that a link is immediately accessible when touched by the invading fluid at one end, neglecting wetting or drying effects, the pinning of the interface due to impurities, and finite contact angles or capillary forces at the pore level.

Mass conservation at each node of the lattice leads to the following set of coupled linear algebraic equations:

$$\sum_j q_{ij} = 0, \quad \text{for } i = 1, 2, \ldots, N^2, \qquad (2)$$

where N^2 is the total number of nodes and the summation j runs over the nearest neighbor nodes of node i. The linear size of the lattice in the x direction is $L = N\ell$. These equations are solved to obtain the node pressures at each time step. In order to simulate the dynamics of viscous invasion, we neglect the effects of fingers in each link containing both phases and consider an abrupt saturation profile along its axial direction. In this way, we can define an interface inside the link separating the oil and the invading fluid. This interface is an approximation and should not be confused with a meniscus in a pore. Then, we allow those interfaces to displace by a length, $\Delta x_{ij} = q_{ij} \Delta t_{\min}/A$, where $\Delta t_{\min}$ is the minimum time, among all links containing both phases, necessary for the invading fluid to reach the end of a link. When an interface reaches the end of a link, reaching a pointlike node, it is instantaneously transferred to those neighbor links whose pressure differences allow for oil displacement. To avoid multiple interfaces in a single link the following rule is adopted. When a third interface appears in a link, these three interfaces are reduced to a single one by merging bubbles of the same phase, so that the phase volume in each link is conserved. The unphysical jumps on the pressure resulting from this reorganization scheme represent only negligible perturbations due to the small size of the corresponding bubbles [24]. This procedure is executed at each time step until a breakthrough happens, i.e., the invading fluid just reaches the other end of the system.

Here we assume that the viscosity of the oil phase typically obeys an exponential dependency on the inverse of temperature,

$$\mu_o = \mu_r e^{B/T}, \qquad (3)$$

where μ_r and B are physicochemical parameters, in units of viscosity and temperature, respectively. The parameter B controls the oil viscosity dependency on temperature. One calls a fluid "heavy oil" if B is high and "light oil" if B is small.

In order to impose a temperature gradient across the medium, different temperatures are assigned to the left (inlet), T_{in}, and right (outlet), T_{out}, boundaries of the lattice and we assume, then, a linear temperature variation from inlet to outlet. This imposed gradient is constant in time, which is analogous to assume that the thermal conductivities of both fluids are negligible compared to that of the rock. Our results are expressed in terms of a dimensionless temperature, $\Delta T' = \Delta T / T_r$, where $\Delta T = T_{\mathrm{in}} - T_{\mathrm{out}}$ and T_r is a reference temperature defined here as the reservoir temperature without heating. Our simulations are performed for temperature differences in the range $-4 \leqslant \Delta T' \leqslant 4$. Negative values of $\Delta T'$ represent a cold injection which is not of technological interest, but can help to understand the nature beyond the fluid displacement under a temperature gradient.

In our approach, ℓ and T_r represent adjusting parameters which one can use for practical applications. For example, if we consider $T_r = 20\,^\circ\mathrm{C}$ and $\ell = 10\,\mathrm{cm}$, the temperature gradient, $\Delta T / L$, varies from 0 to $0.1\,^\circ\mathrm{C/cm}$ as $\Delta T'$ changes from 0 to 4, respectively, with a lattice size of $N = 80$ nodes. By also considering a permeability value of $k = 10\,\mathrm{D}$, $B/T = 3$, $\mu_r = 1\,\mathrm{cp}$, and a pressure gradient of 1 atm/cm, we obtain from Eq. (1) an oil flow velocity $v \approx 4\,\mathrm{cm/min}$. For a typical value of the interfacial tension of the oil (e.g., $\gamma = 20\,\mathrm{dyn/cm}$), the corresponding capillary number can be calculated as $\mathrm{Ca} = 5 \times 10^{-3}$ which is moderately high [29], meaning that the capillary forces can be considered negligible compared to the viscous ones.

In the next section, we show results for the two different cases of the viscosity ratio. In both, μ_o is given by Eq. (3), while μ_{inv} is constant, i.e., independent of the temperature. This can be justified since, for example, water, which is a typical invading fluid, has a viscosity that hardly changes, compared to many types of oils, for common operational temperature intervals.
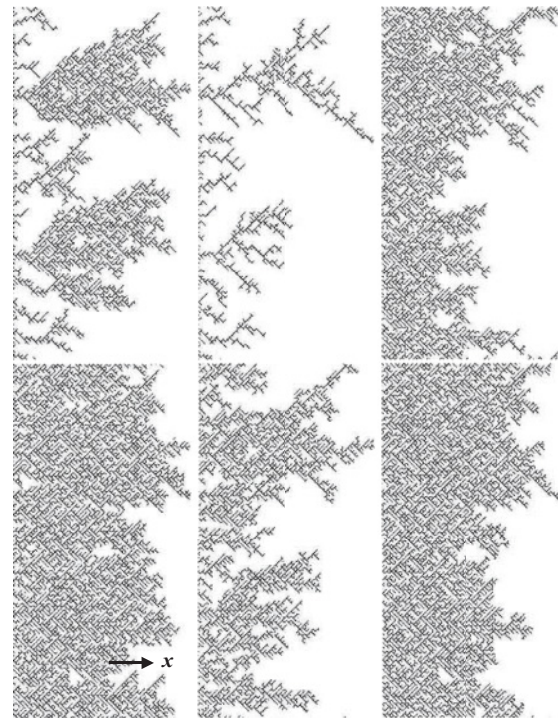

FIG. 1. Snapshots of the invading fluid near breakthrough for the finite viscosity ratio case, using distinct types of oil and temperature differences. All patterns have been generated with the same distribution of permeability for the random links and $N = 80$. From top to bottom, B' changes from 7 to 3, while from left to right, $\Delta T'$ assumes the values -4, 0, and 4.
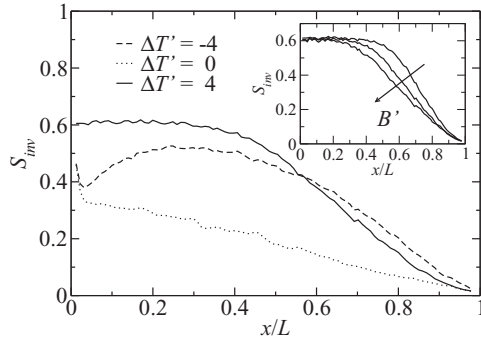
FIG. 2. Near-breakthrough saturation of the invading fluid for the finite viscosity ratio case. The curves correspond to three values of the temperature difference, $\Delta T' = -4$, 0, and 4, $B' = 5$, and $N = 80$. In the inset, we also show the near-breakthrough saturation behavior, but for a fixed value of $\Delta T' = 4$ and $B' = 3$, 5, and 7.

III. RESULTS

In this section, we study the patterns of the invaded region and the percentage of recovered oil when an external fluid with unity viscosity is injected into the medium. We also assume a unity value for μ_r in Eq. (3). According to our model, the viscosity ratio, μ_o/μ_{inv}, has a finite value which changes on x direction, if $\Delta T'$ is different from zero. In Fig. 1 we show six different patterns of the invading fluid with the same distribution of random links for different values of $\Delta T'$ and B', where $B' = B/T_r$. From top to bottom we change B' from 7 to 3, while from left to right $\Delta T'$ assumes the corresponding values of -4, 0, and 4. We clearly observe that either decreasing B' or for positive values of $\Delta T'$, the invading patterns become more compact.

In the isothermal case, $\Delta T' = 0$, the oil viscosity is a constant depending only on B'. For a heavy oil ($B' = 7$), we can see finger patterns appearing in the invaded region. When $\Delta T' > 0$, the viscosity ratio is small on the left side of the lattice and becomes larger as the invading fluid penetrates in the x direction. First, the front advances compactly but at some time, a finger appears and grows faster until it reaches the other end of the lattice. In the opposite case, when $\Delta T' < 0$, fingers appear initially and then become broader. For $B' = 3$, the changes in the viscosity ratio due to the temperature difference suppress the appearance of fingers.
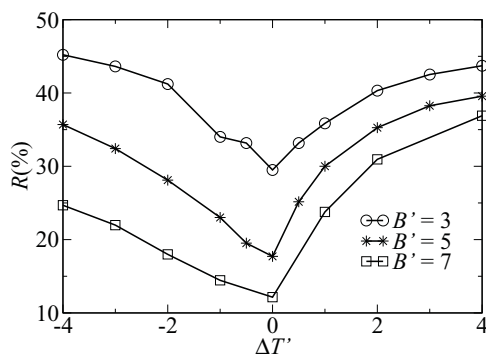

FIG. 3. Percentage of recovered oil versus $\Delta T'$ for the finite viscosity ratio case using three different values of B' and $N = 80$.
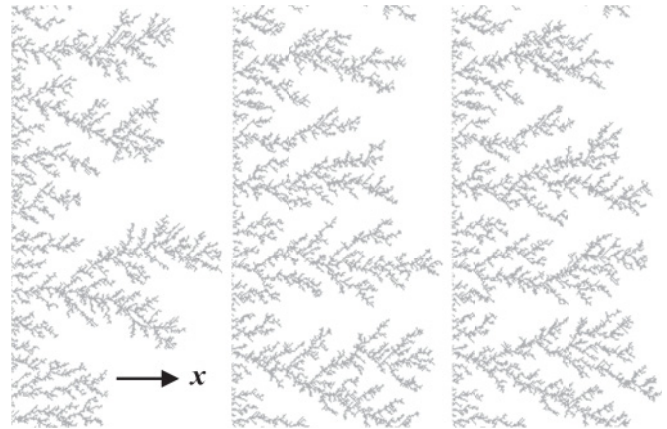

FIG. 4. Snapshots of the invading fluid near breakthrough for the infinite viscosity ratio case. All patterns have been generated with the same distribution of permeability for the random links $B' = 5$ and $N = 256$. From left to right, $\Delta T' = -4$, 0, and 4.

For each set of parameters, we perform simulations with 50 realizations of the disordered porous media, to obtain average values of both the invading fluid saturation and the percentage of recovered oil at the breakthrough. In Fig. 2, we show the near-breakthrough saturation profile of the invading fluid for different values of $\Delta T'$ and B'. We observe that for a positive $\Delta T'$ the saturation profile has a plateau before it starts decreasing in the x direction. However, for a negative $\Delta T'$, finger patterns in the beginning of the lattice produce a dip in the saturation profile close to the inlet. The percentage of recovered oil versus $\Delta T'$ is shown in Fig. 3 for three different values of B'. We see that, despite heavy oil recovery being lower, all types of oil tend to the recovery performance for high values of $\Delta T'$.

Now we study the recovery of an oil that is much heavier than the invading fluid, i.e., for the case of an extremely large viscosity ratio, $\mu_o/\mu_{inv} \to \infty$. This idealized condition is implemented here by considering that the pressure in the invaded fluid immediately adjusts to the injection pressure, i.e., the invading fluid is inviscid. This simplification allows us to simulate bigger lattice sizes, since we need to solve Eq. (2) only for noninvaded sites.
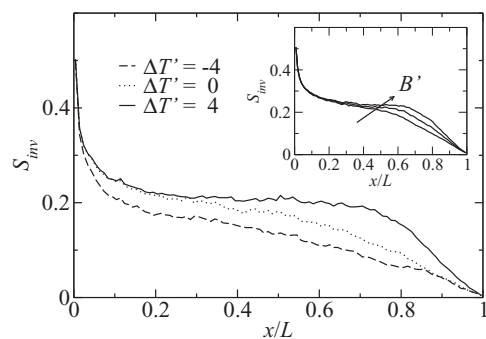

FIG. 5. Near-breakthrough saturation of the invading fluid for the infinite viscosity ratio case. The curves correspond to three values of the temperature difference, $\Delta T' = -4$, 0, and 4, $B' = 5$, and $N = 256$. In the inset, we also show the near-breakthrough saturation behavior, but for a fixed value of $\Delta T' = 4$, and $B' = 1$, 3, and 5.
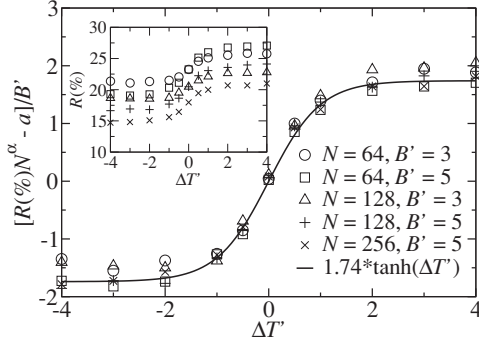
FIG. 6. Percentage of recovered oil versus $\Delta T'$ calculated in the infinite viscosity ratio case, for different values of N and B'. In the main plot, after proper rescaling, we show that these curves collapse on top of each other and can all be fitted to a hyperbolic tangent function. In the inset, we show the same results before rescaling.

In this case, the observed patterns of the interface are always viscous fingeringlike, as shown in Fig. 4, for $\Delta T' = -4$, 0, and 4, with $B' = 5$ and $N = 256$. For $\Delta T' = 0$, these patterns show fingers which agree with well known two-phase displacement patterns with infinite viscosity ratio [30,31]. We can also see that different patterns occur for different values of $\Delta T'$. The reason for this behavior is that, despite the inviscid characteristic of the defending fluid, the oil viscosity has a finite value given by Eq. (3) which falls as the temperature is raised. Then the number of longer fingers for $B' = 5$ increases with $\Delta T'$ as shown Fig. 4. This observation is also valid for $B' = 1$ and 3 (not shown), and therefore represents a standard behavior in the case of infinite viscosity ratio.

For each set of parameters, we averaged over 100 realizations to obtain the invading fluid saturation and the percentage of recovered oil. The near-breakthrough saturation profile of the invading fluid is shown in Fig. 5 for different values of the relevant parameters. For a negative value of $\Delta T'$, the saturation profile always decays in the x direction. However, for a positive $\Delta T'$, we can identify a region in the center of the medium with approximately constant saturation. The extension of this region increases with B' because heavier oils create slower and
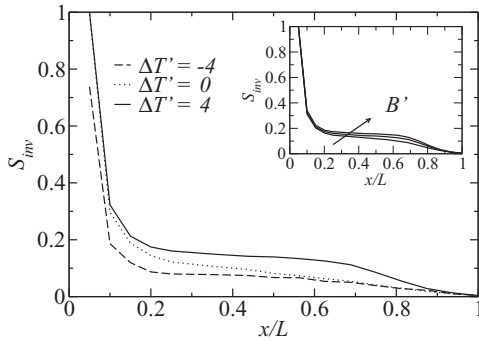

FIG. 7. Near-breakthrough saturation profile of the invading fluid penetrating in a cubic lattice for the case of infinite viscosity ratio. The curves are the results of simulations for $\Delta T' = -4$, 0, and 4, with parameter $B' = 5$ and system size $N = 20$. In the inset, we also show the near-breakthrough saturation behavior, but for a fixed value of $\Delta T' = 4$ and $B' = 3$, 5, and 7.
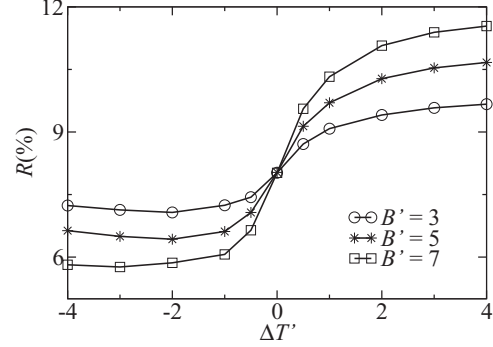

FIG. 8. Dependence of the percentage of recovered oil on the temperature difference $\Delta T'$ or different values of B' on a cubic lattice with $N = 20$ for infinite viscosity ratio.

wider fingers, which tend to make the invasion patterns more compact.

In the inset of Fig. 6, the percentage of recovered oil $R(\%)$ versus $\Delta T'$ is shown for different values of N and B'. The main plot shows that, after rescaling, these curves collapse on top of each other and can be closely described by a hyperbolic tangent function in the form

$$R(\%) = \frac{a + bB' \tanh(\Delta T')}{N^\alpha}, \qquad (4)$$

with parameters $a = 51.11$ and $b = 1.74$ obtained through the best nonlinear fit to the data. The exponent α is found to be about 0.2 and can be computed as $\alpha = d - d_f$, where $d = 2$ is the Euclidean dimension of the lattice and d_f is the fractal dimension, which is found to be 1.8 for our system. The results show that above a certain value of temperature difference, $\Delta T' \approx 2$, no relevant change in $R(\%)$ is observable anymore for all types of oil. This means that a too strong temperature gradient can be an unnecessary cost to the recovery process.

Finally, we also performed simulations with our model in the infinite viscosity ratio regime using a more realistic three-dimensional porous medium substrate. More precisely, we obtained results for a cubic lattice with size $N = 20$ and averaged over 100 realizations for several values of B' and $\Delta T'$. As shown in Figs. 7 and 8, the saturation profiles and the recovery performance of the system, respectively, remain basically the same as compared to the results found for two-dimensional porous media models (for comparison, see Figs. 5 and 6). This qualitative similarity reinforces the validity of our approach as a way to increase the efficiency of the recovery process by means of a temperature gradient.

IV. CONCLUSIONS

In summary, the main purpose here was to investigate how the front between two immiscible fluids propagates in a model porous medium as a function of the ratio of their viscosity and under the influence of an imposed global temperature gradient. An obvious technological application of our study would be to enhance the recovery efficiency of oil being pushed by hot water in a petroleum reservoir. In our simulations, this has been accomplished by explicitly coupling the oil viscosity with the inverse of temperature locally in terms of a simple exponential

dependence. We thus proceeded with the displacement of several types of oil through many realizations of disordered porous medium and subjected to a range of distinct temperature differences.

Two different regimes of viscosity ratio have been studied. In the first, oil viscosity changes with temperature and the viscosity ratio is always finite, but can vary over several orders of magnitude. In the second regime, oil is assumed to be "heavy" in the sense that it is extremely viscous when compared to the invading fluid, even if a maximum temperature difference is applied, hence the viscosity ratio can be considered as infinite. We find that the best conditions for recovery are significantly dependent on the adopted regime. In the finite viscosity ratio case, an oil with a viscosity that is only weakly dependent on the temperature is better recovered, independent of the strength or sign of the gradient. Also in this case, different invasion patterns can be observed as the viscosity ratio changes, namely, we find fronts that are compact, unstable, and sometimes a mix of both.

In the case of infinite viscosity ratio, oil recovery increases with the exponential parameter B if the temperature difference is positive. Moreover, recovery is found to follow a hyperbolic tangent behavior on the temperature difference and the best recovery is obtained for positive temperature gradients (hot-water injection). It would be interesting to verify our predictions with experimental results. Since field experiments in this area are usually difficult and expensive, it would be advisable to run laboratory-size experiments in which interface patterns are dynamically registered and the recovered volume is systematically measured while a viscous fluid is displaced by a less viscous one in a porous medium under the influence of temperature gradients.

[1] M. Prats, *Thermal Recovery*, SPE Monograph Series (SPE, AIME, Richardson, 1982).

[2] B. C. Craft and M. F. Hawkins, *Applied Petroleum Reservoir Engineering*, 2nd ed. (Prentice Hall, New Jersey, 1991).

[3] G. Moore, R. Mehta, and M. Ursenbach, J. Cdn. Pet. Tech. **41**, 16 (2002).

[4] F. Civan, Pet. Sci. Technol. **24**, 699 (2006).

[5] A. T. Turta and A. K. Singhal, J. Cdn. Pet. Technol. **43**, 29 (2004).

[6] M. I. Kuhlman, SPE 86954 (2004).

[7] J. S. Andrade, A. D. Araújo, S. V. Buldyrev, S. Havlin, and H. E. Stanley, Phys. Rev. E **63**, 051403 (2001).

[8] M. Ferer, G. S. Bromhal, and D. H. Smith, Adv. Water Resour. **30**, 284 (2005).

[9] M. Ferer, W. N. Sams, R. A. Geisbrecht, and D. H. Smith, Phys. Rev. E **47**, 2713 (1993).

[10] J. S. Andrade, M. P. Almeida, J. Mendes Filho, S. Havlin, B. Suki, and H. E. Stanley, Phys. Rev. Lett. **79**, 3901 (1997).

[11] P. R. King, J. S. Andrade, S. V. Buldyrev, N. Dokholyan, Y. Lee, S. Havlin, and H. E. Stanley, Physica A **266**, 107 (1999).

[12] H. Auradou, K. J. Måløy, J. Schmittbuhl, A. Hansen, and D. Bideau, Phys. Rev. E **60**, 7224 (1999).

[13] J. S. Andrade, U. M. S. Costa, M. P. Almeida, H. A. Makse, and H. E. Stanley, Phys. Rev. Lett. **82**, 5249 (1999).

[14] Y. Lee, J. S. Andrade, S. V. Buldyrev, N. V. Dokholyan, S. Havlin, P. R. King, G. Paul, and H. E. Stanley, Phys. Rev. E **60**, 3425 (1999).

[15] M. Sahimi, Rev. Mod. Phys. **65**, 1393 (1993).

[16] J. S. Andrade, S. V. Buldyrev, N. V. Dokholyan, S. Havlin, P. R. King, Y. Lee, G. Paul, and H. E. Stanley, Phys. Rev. E **62**, 8270 (2000).

[17] A. D. Araújo, W. B. Bastos, J. S. Andrade, and H. J. Herrmann, Phys. Rev. E **74**, 010401(R) (2006).

[18] R. Lenormand, E. Touboul, and C. Zarcone, J. Fluid Mech. **189**, 165 (1988).

[19] A. D. Araújo, J. S. Andrade, and H. J. Herrmann, Phys. Rev. Lett. **97**, 138001 (2006).

[20] M. Hashemi, B. Dabir, and M. Sahimi, AIChE J. **45**, 1365 (1999).

[21] C. Lu and Y. C. Yortsos, AIChE J. **51**, 1279 (2005).

[22] C. A. Lu and Y. C. Yortsos, Phys. Rev. E **72**, 036201 (2005).

[23] C. Lu and Y. C. Yortsos, Ind. Eng. Chem. Res. **43**, 3008 (2004).

[24] E. Aker, K. J. Måløy, A. Hansen, and G. G. Batrouni, Transp. Porous Media **32**, 163 (1998).

[25] E. Aker, K. J. Måløy, and A. Hansen, Phys. Rev. E **58**, 2217 (1998).

[26] T. Ramstad, A. Hansen, and P. E. Øren, Phys. Rev. E **79**, 036310 (2009).

[27] H. A. Knudsen and A. Hansen, Eur. Phys. J. B **49**, 109 (2006).

[28] M. Sahimi, *Flow and Transport in Porous Media and Fractured Rock* (VCH, Boston, 1995).

[29] J. Feder, *Fractals* (Plenum, New York, 1988).

[30] G. M. Homsy, Annu. Rev. Fluid Mech. **19**, 271 (1987).

[31] J.-D. Chen and D. Wilkinson, Phys. Rev. Lett. **55**, 1892 (1985).